

Ab initio calculations of structural and electronic properties of CdTe clusters

Somesh K. R. Bhattacharya and Anjali K shirsagar^{*}

Department of Physics, University of Pune, Pune 411 007, India.

(Dated: February 8, 2020)

We present results of a study of small stoichiometric Cd_nTe_n ($1 \leq n \leq 6$) clusters and few medium sized non-stoichiometric Cd_mTe_n ($(m;n = 13;16;19); (m \neq n)$) clusters using the Density Functional formalism and projector augmented wave method within the generalized gradient approximation. Structural properties viz. geometry, bond length, symmetry and electronic properties like HOMO-LUMO gap, binding energy, ionization potential and nature of bonding etc. have been analyzed. Medium sized non-stoichiometric clusters were considered as fragments of the bulk with T_d symmetry. It was observed that upon relaxation, the symmetry changes for the Cd rich clusters whereas the Te rich clusters retain their symmetry. The Cd rich clusters develop a HOMO-LUMO gap due to relaxation whereas there is no change in the HOMO-LUMO gap of the Te rich clusters. Thus, the symmetry of a cluster seems to be an important factor in determining the HOMO-LUMO gap.

PACS numbers:

I. INTRODUCTION

Semiconductor nanoparticles or Quantum Dots (QDs), in particular of II-VI materials, have received tremendous attention during the last two decades owing to their unusual physical properties and wide range of applications¹. A systematic study of QDs is useful to understand the evolution of their physical and chemical properties with size. Moving from a molecule to bulk, one can observe a range of variation of fundamental properties. This size dependent effect, however, is most significant for small sized clusters and is attributed to the different geometry of clusters in comparison to the bulk. Quantum confinement of electronic states and large surface to volume ratio modify the properties of these clusters. In bare clusters, unsaturated bonds lead to peculiar structural and electronic properties like surface reconstruction, formation of new cleavage planes etc.

The differences in the structural properties also affect the electronic properties of the QDs. In bulk systems one observes quasi-continuous electronic levels forming bands whereas in clusters the electronic levels are discrete. Apart from the structural and electronic properties, other properties like the thermodynamic and optical properties too differ significantly for clusters as compared to bulk^{2,3}.

Among the II-VI semiconductors, CdX ($X = S, Se, Te$) have potential application in optical and optoelectronic devices. CdTe nanoclusters, in particular, are used in optical sensors. Multilayered CdTe with poly(diallyldimethylammonium chloride) are electro and photoactive and hence are used in neuroprosthetic devices⁴. Self assembled CdTe nanodots have high efficiency in terms of photoluminescence and hence are very good for the purpose of making LEDs. CdTe and Au nanohybrid materials have photoluminescence variation depending upon environmental condition like temperature, ionic strength, solvents and hence are used as biosensors⁵.

We present here Density Functional Theory (DFT) based calculation of some small, Cd_nTe_n ($1 \leq n \leq 6$) and

few medium sized Cd_mTe_n ($(m;n = 13;16;19) (m \neq n)$) clusters. Both Cd and Te in bulk phase exist in hexagonal structure with c/a ratio 1.89 and 1.33 respectively⁶ whereas CdTe in bulk has only zincblende structure unlike some of other II-VI semiconductors and has a direct band gap of 1.56 eV at 300K⁷.

Study of small clusters is challenging due to lack of experimental structural information and increased degree of freedom. Very small clusters (containing up to 8-10 atoms) exhibit symmetry and have only a few possible geometries. On the other hand, medium sized clusters can be considered as fragments of bulk possessing the same structural symmetry as that of the bulk⁸. To the best of our knowledge, so far no ab-initio calculations have been reported on CdTe QDs. We compare our results for small CdTe QDs with those of CdS and CdSe wherever available.

A variety of methods based on ab-initio DFT⁹, quantum chemistry methods¹⁰ like Hartree-Fock, Gaussian etc. and approximate methods^{2,6} like tight-binding method¹² have been widely used for II-VI semiconductor nanoclusters to study the structural, electronic and optical properties.

II. METHODOLOGY AND COMPUTATIONAL DETAILS

The first step for calculating the cluster properties is the determination of the lowest energy conformation. Structural determination for clusters is very complicated considering the coordination. Existence of several such conformations and multiple minima in the potential energy surface enormously complicate the problem making it almost impossible to decide by direct calculation the lowest energy conformation for clusters.

In this work we have used Born-Oppenheimer molecular dynamics² within the Kohn-Sham density functional framework¹³. The electronic structure is calculated self-consistently using projector augmented wave

(PAW) method¹⁴ as implemented in VASP package¹⁶ within the framework of GGA instead of Vanderbilt ultrasoft pseudo-potential (USPP)¹⁷ as it provides better first principle simulations as compared to USPP¹⁴. In pseudo potential methods, the effect of core electrons and nuclei is replaced by an effective ionic potential and only the valence electrons which are directly involved in chemical bonding are considered.

Various parameterizations have been used for different exchange-correlation potentials in the DFT formalism^{23?} in the literature. It has been reported that generalized gradient approximation (GGA) gives much better results for binding energy and band gap as compared to local density approximation (LDA)² and therefore we have used GGA, as developed by Perdew-Berke-Emzerhof (PBE)¹⁸ for our calculation. PBE is known to improve total energy and molecule atomization energy and therefore the electronic properties as compared to PW91 and the results agree with that of the experiments very well.

The geometry of small clusters varies significantly from that of the bulk. We have chosen several possible initial geometries by exploiting the symmetry considerations and by exchanging the positions of anionic and cationic atoms. The number of initial structures is small for very small clusters. But for clusters with 10-12 atoms, lot many configurations have been used to determine the lowest energy structure.

For structure optimization we have used a super-cell of size $a = 25\text{\AA}$ and the plane wave cut-off was set to be 274.3 eV. These values are chosen after performing calculations for different cell sizes and cut-off energies. We have employed conjugate gradient (CG) technique implemented via Kossiga algorithm (special Davidson block iteration scheme) for optimizing geometry.

The valence electron configuration used for Cd and Te is $5s^2 4d^{10}$ and $5s^2 5p^4$ respectively. The 4d levels in Te atom are well separated from the 5s level and hence can be included in the core.

CdTe in bulk has zincblende (ZB) structure with T_d symmetry. Therefore for medium sized non-stoichiometric clusters $Cd_m Te_n$ ($m \neq n$), the initial geometry was considered as a fragment of the ZB structure. The size of the super-cell was chosen to be $a = 30\text{\AA}$ which is sufficiently large to minimize inter-cluster interactions even for the largest cluster size we consider in this work. In all the structure minimizations, the force and energy convergence obtained was 10^{-3} eV/Å and 10^{-4} eV respectively.

III. RESULTS AND DISCUSSIONS

A. Structural properties of $Cd_n Te_n$

The geometries for lowest energy (LE) of $Cd_n Te_n$ obtained by CG are shown in figure 1 and the first local minima (FLM) in figure 2. It is interesting to note that

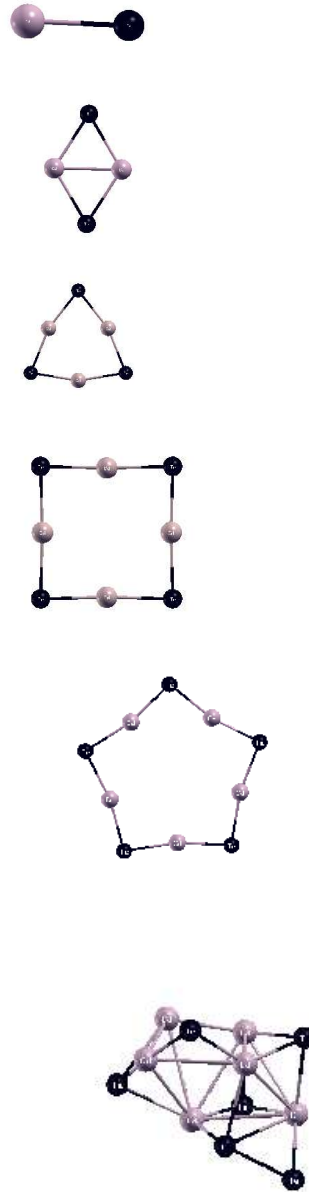


FIG. 1: Lowest energy configuration of $Cd_n Te_n$ for (1 - n 6) The grey atoms are Cd and the black atoms are Te.

for all the calculated lowest energy structures, the chalcogenide atoms are at the peripheral positions. This is a direct consequence of Coulomb repulsion between the lone-pairs situated on the chalcogenide atoms which is minimized by separating the chalcogenide atoms towards the peripheral position. As expected, the ground state structures of these CdTe clusters do not resemble the bulk phase.

CdTe dimer is a linear molecule with bond length of 2.57Å and belongs to C_{1v} point group. For $Cd_2 Te_2$, $Cd_3 Te_3$, $Cd_4 Te_4$, $Cd_5 Te_5$ and $Cd_6 Te_6$, there are two pos-

sible lowest energy configurations within the energy difference of 0.11eV, 0.22eV, 0.04eV, 0.05eV and 0.09eV, per atom respectively. Except for Cd₆Te₆, the lowest energy geometry is a planar ring structure. Cd₂Te₂ has LE as the rhombic structure and a square planar structure as FLM. The LE and FLM belong to D_{2h} and C_{2v} point group respectively. Cd₃Te₃ has triangular structure (D_{3h} point group) as LE configuration and another planar structure (C_s point group) as the FLM. No three dimensional (3D) stable geometry is obtained for n = 2;3. For Cd₄Te₄, the square planar (D_{4h} point group) geometry is obtained for LE and 3D tetrahedral structure (T_d point group) as FLM. Cd₅Te₅ is a planar pentagon (C_s point group) in LE and a non-symmetric 3D structure as FLM. A transition from planar LE to 3D LE occurs for n = 6. This is attributed, as explained later, to the tendency of achieving higher coordination without putting too much strain on the bond angle. All the planar structures show a coordination of 2 for all the atoms in these clusters, except for the FLM of Cd₃Te₃.

The geometries obtained for the CdTe clusters are quite similar to those of corresponding CdS and CdSe clusters upto n = 4²³. However, the geometries of Cd₅Te₅ and Cd₆Te₆ are very different from the CdS and CdSe counterparts²³. This difference may be attributed to the fact that we have included 4d of Cd in the valence configuration in the present study. The necessity of including 4d electrons of the cations in the valence configuration has been emphasized by Wei and Zunger¹⁹.

As we move from planar to 3D structure the coordination of atoms increases from 2 to 3. The 3D structures of Cd₄Te₄, Cd₅Te₅ and Cd₆Te₆ can be considered to be made up of small cluster units namely Cd₂Te₂ and Cd₃Te₃.

A comparison of Cd_nTe_n clusters with Cd_n²⁰ and S_n²¹ and Se_n clusters brings out drastic differences. Three dimensional structures are more favorable in Cd clusters as compared to CdTe clusters where planar structure is favored even for 10 atom cluster.

Figure 3 shows the variation of average Cd-Te bond length with the number of atoms in the clusters. The near neighbour (nn) distance for CdTe bulk is 2.81Å. As evident from fig. 3, these clusters have an average bond length less than that of bulk. This is due to incomplete coordination in these clusters on account of very small number of atoms. The bond length of CdTe dimer is the smallest. In fact, the smallest Cd-Te bond length remains almost constant in these clusters for n = 3-6 (not shown in figure). The average Cd-Te bond length shrinks with increase in n in planar structures (n = 2-5) and increases in going from planar to 3D structures.

Surface studies²² on heteropolar covalent and ionic semiconductors have identified quantum mechanical electron-electron Coulomb repulsion, hybridization effects and classical Coulomb attraction between anion and cation as competing factors in deciding the stability of the surface. The last factor seems to be more important with only 3 neighbours for atoms on the surface. Opti-

mum energy gain is achieved when the distance between anion and cation is as small as possible. Thus shorter bonds are more ionic in nature. We therefore expect that CdTe dimer will have more ionic character as compared to other clusters. In Cd₂Te₂, there exist a covalent bond between Cd-Cd which accounts for an increase in average Cd-Te bond length. As explained later from the charge density plots, there are no covalent bonds between either Cd-Cd or Te-Te in other planar structures (n = 3-5). Therefore, the average Cd-Te bond length is smaller in these clusters. In Cd₆Te₆, bonds between similar atoms appear as a result the average Cd-Te bond length increases.

Cd-Cd bond length in Cd₂Te₂ is smaller (2.87Å) than in Cd dimer (3.47Å). The average Cd-Cd bond length is same in Cd₃Te₃ and Cd₃. However, it is larger in Cd_nTe_n as compared to Cd_n for 3 < n < 6. In contrast, average Te-Te bond length is significantly larger in CdTe clusters as compared to pure Te clusters as expected due to lone pair repulsion. Also it does not appreciably change with n.

Average Te-Cd-Te bond angle increases from 107.2° in Cd₂Te₂ to nearly 180° in Cd₄Te₄. The angle further opens up in Cd₅Te₅. In Cd₆Te₆, all the Te-Cd-Te angles are smaller than linear angle as a consequence of 3D structure. Thus we see that smaller clusters have a tendency to form linear Te-Cd-Te bonds resulting in planar structures with coordination of 2 and as higher coordination number takes over, a transition from planar to three dimensional structure results for stable geometry.

All the clusters are found to be stable against fragmentation into smaller clusters.

B. Electronic properties of Cd_nTe_n

Figures 4 and 5 show the variation in the highest occupied molecular orbital (HOMO) - lowest unoccupied molecular orbital (LUMO) gap (E_g) and binding energy per Cd-Te unit with the number of Cd-Te units in the cluster.

$$E_b = [n E(Cd) + E(Te)] - E(Cd_n Te_n) \quad (1)$$

The trends seen in these two curves are found to be similar in CdS and CdSe²³ and the stability of clusters can be inferred from them. However, we do not see any such correlation for the clusters studied in the present work. Another property of interest for discussing the stability of clusters is the vertical detachment energy (VDE), shown in Fig. 6.

It is seen that Cd₅Te₅ is more stable compared to its neighbours. It may be mentioned that the number of electrons in this system are 90 which matches with the shell closing number for jellium-like systems.

We have calculated the electron affinity by performing two self-consistent calculations for electronic system without allowing any change in the geometry. Figure 7 shows the plot of electron affinity of various CdTe clusters.

In bulk CdTe, the bonding is mostly covalent as the atomic number and hence the atomic radii for Cd and Te are very close. As a result, the Coulombic forces between the two species are balanced very well. However due to difference in electronegativity of Cd and Te, the bonding has some ionic character even in the bulk.

(The grey atoms are Cd and black atoms are Te.)

We show total charge density iso-surface plots for CdTe dimer and Cd₂Te₂ cluster in Figs. 8 and 9 respectively revealing covalent bonding. From the electron density plots we see building up of charge between the atoms and it is directional. Hence the bonding is covalent in nature. Similar charge density distribution occur for other clusters too. No Cd-Cd or Te-Te near neighbour bonds are seen to be formed. The charge density plots for CdS and CdSe²³ show that the bonding has some ionic character and is not purely covalent. Ionicity in bonding is more in CdS than in CdSe because of smaller atomic radius of sulphur. Ionicity is expected to be still smaller in CdTe.

An analysis of charge inside atomic spheres with covalent radii shows that the distribution of charge in the Cd and Te spheres is almost same for planar structures for $n = 3 - 5$. There is more charge localization in planar structures in comparison to CdTe dimer, Cd₂Te₂ and the 3D structures.

A more detailed information regarding the bonding in these clusters can be obtained from the partial charge density plots of the molecular orbitals (MOs) in these clusters.

From Figs. 10 and 11 it is evident that the HOMO consists of purely Te p and in the LUMO the Cd s and p hybridize to give a sp-hybrid orbital which in turn forms a sigma bond with the Te p orbital.

The plots for HOMO-LUMO of Cd₃Te₃ are shown in figure 12 and 13. The HOMO is only Te p levels whereas the LUMO is sp-hybrid of Cd forming a sigma bond with Te p as in case for dimer. Figure 13 also shows the delocalisation of the charge density in the central region of the clusters indicating a semi-metallic character in the bonding. Thus, these systems will favour electron addition as is also evident from Fig. 7. For other clusters the partial charge density for HOMO and LUMO have similar nature.

As seen from the MO charge distribution of HOMO as one goes from $n = 2$ to $n = 6$, an enhancement in delocalisation results accounting for a steady decrease in the VDE as shown in Fig. 6.

In Fig. 14 we show the one-electron energies for all the CdTe clusters and the atomic levels of Cd and Te. The Cd s and the Te p levels lie in the same energy window in the atomic case. Consequently, an intermixing of these orbitals occur in the clusters. A fat band analysis of the CdTe bulk band structure (not shown here) using full potential linear augmented plane wave method reveals similar intermixing of orbitals. Thus, the bulk type mixing of the orbitals is retained in these clusters. The movement of the the HOMO and LUMO in these small clusters is quite interesting. As the clus-

ter size increases, the HOMO moves downward whereas the LUMO moves upward resulting in widening of the HOMO-LUMO gap. However, this shift is not uniform. The HOMO moves downward slowly as compared to the LUMO which moves upward rapidly. But for Cd₆Te₆, the HOMO shifts slightly upward and the LUMO shifts downward resulting in a smaller HOMO-LUMO gap as a consequence of planar to 3D transition in geometry.

C. Properties of Cd_mTe_n clusters

CdTe in bulk occurs only in ZB phase however many other II-VI semiconductors have ZB and wurtzite (W) phases possible. There are also reports of size induced phase transitions in ZnS²⁴ and CdS²⁵ nanoparticles. The first coordination for central atom is identical in ZB and W phases. If we consider the trigonal axis [111] in ZB and [001] in W then three near neighbours are identical.

We have, therefore, performed calculations for four larger non-stoichiometric CdTe clusters viz. Cd₁₃Te₁₆ (central atom + 3 neighbouring shells), Cd₁₆Te₁₃, Cd₁₆Te₁₉ (central atom + 4 shells) and Cd₁₉Te₁₆. These clusters have been considered as fragments of the bulk and hence their initial symmetry is T_d as shown in Fig. 16(a) and ??(a).

Cd₁₃Te₁₆ has a central Cd atom. The relaxed structure (Fig. 16(b)) has Te-Cd-Te bond angle for the central Cd atom of 109.47°. The average Cd-Te bond length is 2.81Å which is same as that of the bulk. Cd₁₆Te₁₃, (Fig. 16(c)) has a Te atom at the center. The Cd-Te-Cd bond angle for the central Te atom after relaxation is 109.48° and the average bond length for the relaxed structure is 2.84Å. During relaxation the central Te atom pushes the neighboring Cd atoms outward. For Cd₁₆Te₁₉, the relaxed structure (Fig. ??(b)) has Cd-Te-Cd bond angle for the central Te atom of 109.47° and its average Cd-Te bond length is 2.82Å which is again almost same as that of the bulk limit. Cd₁₉Te₁₆ has a Cd atom in the center and its relaxed structure (Fig. ??(c)) has Te-Cd-Te bond angle for the central Cd atom of 91.31° and the average Cd-Te bond length is 2.81Å.

Symmetry of relaxed geometry of these clusters show very interesting features. Initially all the four clusters have tetrahedral symmetry T_d. But upon relaxation only the Te rich clusters retain their T_d symmetry whereas the Cd rich clusters attain lower symmetry structures. The observed symmetry, calculated binding energy per atom, average Cd-Te bond length and HOMO-LUMO gap for the relaxed structures of these clusters have been tabulated in table I. It may be mentioned that the binding energy of CdTe dimer is 0.7630 eV/atom whereas the cohesive energy of CdTe bulk is 4.9 eV.

Comparison of the binding energies of the above clusters clearly indicates that Cd₁₃Te₁₆ and Cd₁₆Te₁₉ are more stable than Cd₁₆Te₁₃ and Cd₁₉Te₁₆. In the former group the Te atoms are on the surface and hence these structures are energetically favoured as discussed

TABLE I: Symmetries, Binding energy, average Cd-Te bond length and HOMO-LUMO gap for Cd_mTe_n ($m \leq n$)

Clusters	Symmetry	Binding energy (eV/atom)	Avg. Cd-Te bond length (Å)	HOMO-LUMO gap (eV)
$Cd_{13}Te_{16}$	T_d	2.13	2.81	0.1951
$Cd_{16}Te_{13}$	C_{3v}	1.95	2.84	0.6595
$Cd_{16}Te_{19}$	T_d	2.14	2.82	0.0881
$Cd_{19}Te_{16}$		1.95	2.81	0.9636

earlier. For the Te rich clusters, the relaxation is not strong enough to break their initial T_d symmetry owing to their higher binding energy as compared to the Cd rich clusters. On the other hand, the Cd rich clusters, being weakly bound, go to lower symmetry structures upon relaxation. A comparison of binding energy per atom for Cd_mTe_n with corresponding Hg_mTe_n clusters⁸ shows a reduction. This is attributed to symmetry allowed pd interactions. The d levels of Hg are closer to Te p levels than Cd. Therefore pd-repulsion induced bond weakening is more in HgTe than in CdTe clusters resulting in a reduction of binding energy.

A very interesting feature observed in the Cd rich clusters is Jahn-Teller distortion. The initial HOMO-LUMO gap for $Cd_{16}Te_{13}$ and $Cd_{19}Te_{16}$ is nearly zero. But upon relaxation, they attain an appreciable HOMO-LUMO gap. This is a clear indication that the energy levels which are nearly degenerate in the initial structure have moved apart during relaxation. Thus, relaxation has destroyed its symmetry resulting in the lifting of degeneracy. On the other hand for the Te rich clusters, the HOMO-LUMO are not degenerate (though close to each other) and thus there is no Jahn-Teller distortion. Similar trend has also been observed in non-stoichiometric HgTe clusters⁸. The Hg rich clusters upon relaxation lose their initial T_d symmetry. As a result, they attain a definite bandgap and a semiconductor to semiconductor transition is observed. Dalpian et. al have shown that symme-

try is an important parameter in deciding the properties of nanoclusters²⁷.

IV. CONCLUSION

The ground state geometries of Cd_nTe_n ($1 \leq n \leq 6$) were calculated using ab-initio DFT. The structures do not resemble that of the bulk phase. The Cd atoms tend to form a core group surrounded by the chalcogenide atoms because of the Coulomb's repulsion of the lone pair of p-electrons on Te. For Cd_nTe_n , ($1 \leq n \leq 5$), the planar geometry is the lowest energy conformation as Te-Cd-Te prefer to form linear bond. But as the number of atoms increases further, higher coordination takes over and three dimensional structures result. Bonding in CdTe clusters is mostly covalent in nature with partial ionic character. The degree of ionicity changes with n . The hybridization of atomic orbitals in these clusters is the same as that in bulk.

The ground state non-stoichiometric clusters, Cd_mTe_n with $(m;n) = 13;16;19$ and $m \leq n$, were calculated using ab-initio DFT with the wavefunction projected to real space. The Te rich clusters with Te atoms on the surface, are found to be more stable than the Cd rich clusters. The symmetry of the cluster plays a vital role in determining its HOMO-LUMO gap. It was found that the Cd rich cluster lose their initial T_d symmetry and attain a large HOMO-LUMO gap as compared to the Te rich clusters.

V. ACKNOWLEDGMENT

We are thankful to the Dept. of Science and Technology, Govt. of India, for their financial support in carrying out this work. We would also like to thank to IUCAA, Pune and Centre for Modelling and Simulation (CMS), University of Pune for allowing us to use their computational facilities.

Electronic address: skb@physics.unipune.ernet.in

^y Electronic address: anjali@physics.unipune.ernet.in

¹ V. L. Colvin, M. C. Schlamp, A. P. Alivisatos, Nature (London) 370, 354 (1994); A. P. Alivisatos, J. Phys. Chem. 100, 13226 (1996).

² S. Ogot, J. R. Chelikowsky, S. G. Louie, Phys. Rev. Lett., 79 1770 (1997); I. Vasiliev, S. Ogot and J. R. Chelikowsky, Phys. Rev. B 65, 115416 (2002) and references therein.

³ A. Shvartsberg (private communication).

⁴ M. Gao et. al, J. Appl. Phys. 87, 5, 2297 (2000).

⁵ Li J et. al, Chem. Commun. (Camb.) 8, 982 (2004).

⁶ N. W. Ashcroft and N. D. Mermin, Solid State Physics, (Holt-Saunders Phil 1981).

⁷

⁸ X. Q. Wang, S. J. Clark and R. A. Abram, Phys. Rev. B 70, 235328 (2004).

⁹ V. S. Gurin, Int. J. Q. Chem. 71, 337 (1999); J-O Joswig et.al, J. Phys. Chem. B 104, 2617 (2000); A. J. Williamson and A. Zunger, Phys. Rev. B 61, 1978 (2000); J. M. Maxtain, J. E. Fowler and J. M. Ugadde, Phys. Rev. A, 61, 053201 (2001).

¹⁰ J. M. Ullu and T. A. Pakkanen, Sur. Sci. 364, 439 (1996).

²⁶ E. Spano, S. Hamad and C. R. Catlow, Journal of Phys. Chem. 13, 107, 10337 (2003).

¹² V. A. Ibe, C. Jouanin and D. Bertho, J. Cryst. Gr. 184/185, 388 (1998); S. Pokrant and K. B. W. Haley, Eur. Phys. J. D 6, 255 (1999).

¹³ P. Hohenberg and W. Kohn, Phys. Rev. 136, B864 (1964);

- W. Kohn and L. J. Sham, *Phys. Rev.* 140, A 1133 (1965).
- ¹⁴ P. E. Blochl, *Phys. Rev. B* 50, 17953 (1994); G. Kresse and J. Joubert, *Phys. Rev. B* 59, 1759 (1999).
- ¹⁵ O. Gunnarsson and R. Jones,
- ¹⁶ Vienna ab initio simulation package, Technische Universität Wien (1999); G. Kresse and J. Furthmüller, *Phys. Rev. B*, 54, 11169 (1996).
- ¹⁷ D. Vanderbilt et. al, *Phys. rev. Lett.* 69, 1982 (1992); D. Vanderbilt et. al, *Phys. Rev. B* 47, 10142 (1993)
- ¹⁸ Perdew et. al, *Phys. Rev. Letters*, 77, no. 18, 3865 (1996).
- ¹⁹ S.-H. Wei and A. Zunger, *Phys. Rev. B* 37, 8958 (1988); *J. Cry. Gr.* 86, 1 (1988).
- ²⁰ J. Zhao, *Phys. Rev. A*, 64, 043204 (2001).
- ²¹ D. Holz, R. O. Jones, R. Car and M. Parrinello, *J. Chem. Phys.* 89, 6823 (1988).
- ²² D. Vogel, P. Krüger and J. Pollmann, *Sur. Sci.* 402-404, 774 (1998).
- ²³ M. C. Tropicovsky and J. R. Chelikowsky, *Journal of Chemical Physics* 114 no. 2, 943 (2001).
- ²⁴ J. Nanda and D. D. Sarna, *J. Appl. Phys.* 90, 2504 (2001).
- ²⁵ T. Namba et. al, *J. Phys. Soc. Jpn.* 66, 1526 (1997); R. Banerjee, R. Jayakrishnan and P. Ayyub, *J. Phys.: Cond. Matt.* 12, 10647 (2000).
- ²⁶ E. Spano, S. Hamad and C. R. Catlow, *Journal of Phys. Chem.*, 13, 107, 10337 (2003).
- ²⁷ G. M. Dalpian, M. L. Tiago, M. L. Puerto and J. R. Chelikowsky, *Nano-Letters*, 6, 501 (2006).

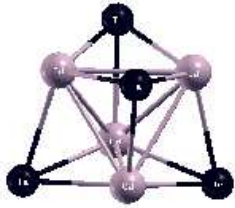
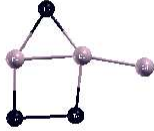


FIG. 2: Geometries of the first local minimum in a of Cd_nTe_n , for $(1 \leq n \leq 6)$.

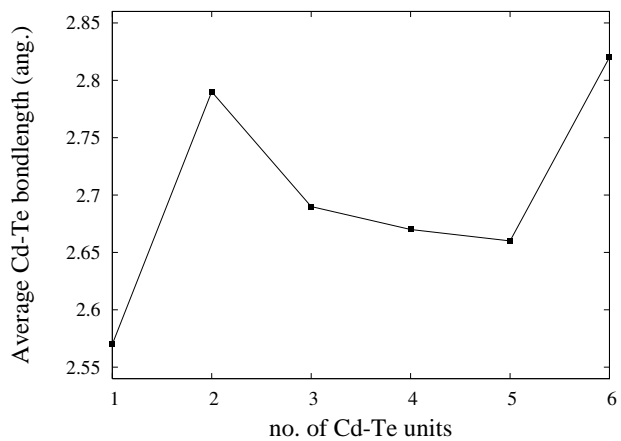


FIG . 3: Average Cd-Te bond length (ang.) vs number of Cd-Te units

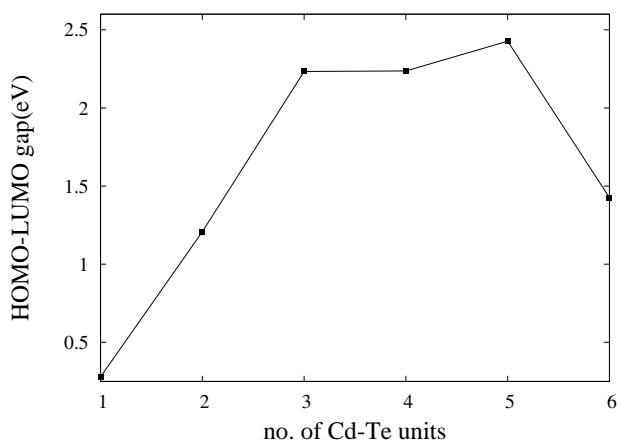


FIG . 4: HOMO-LUMO gap (eV) vs number. of Cd-Te units

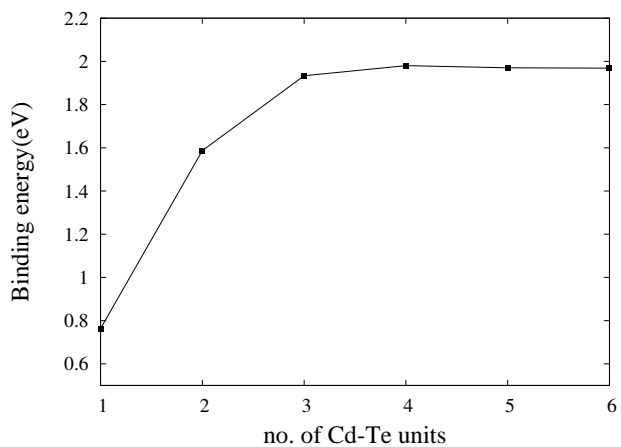


FIG . 5: Binding energy (eV) vs number of Cd-Te units

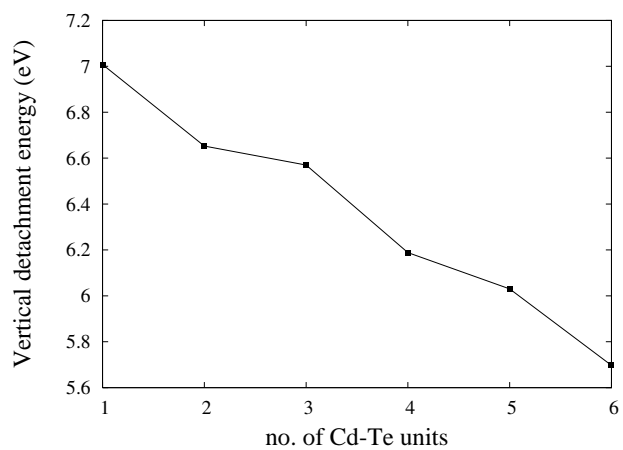


FIG .6: Vertical detachment energy (eV) vs number of Cd-Te units

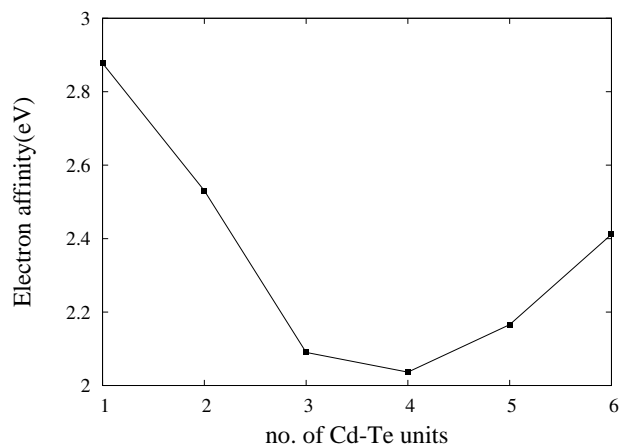


FIG .7: Electron affinity vs number of Cd-Te units

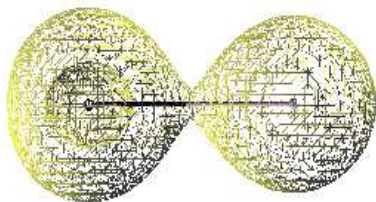


FIG .8: Charge density of CdTe dimer

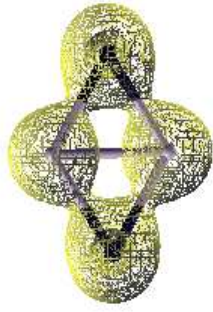


FIG . 9: Charge density of Cd_2Te_2

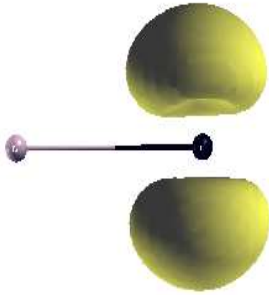


FIG . 10: Plot of partial charge density of HOMO for CdTe dimer

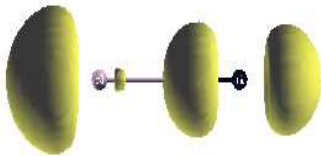


FIG . 11: Plot of partial charge density of LUMO for CdTe dimer

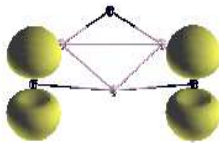


FIG . 12: Plot of partial charge density of HOMO for Cd_3Te_3

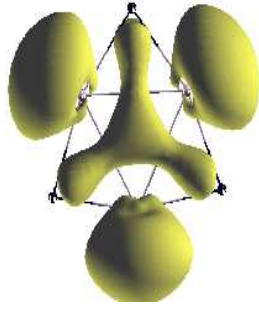


FIG .13: Plot of partial charge density of LUMO for Cd_3Te_3

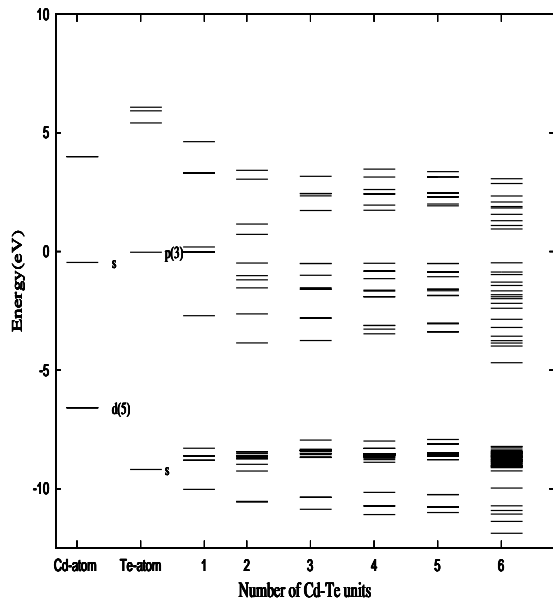
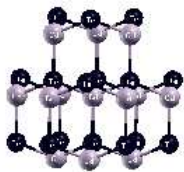
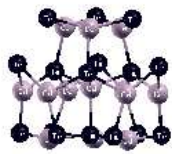


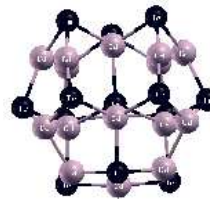
FIG .14: Energy level diagram of CdTe clusters



(a) $Cd_{13}Te_{16}$: initial



(b) $Cd_{13}Te_{16}$: relaxed

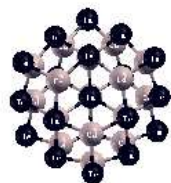


(c) $Cd_{16}Te_{13}$: relaxed

FIG .15: Sideview of the initial and relaxed geometries



(a) C_{d16}T_{e19} : initial



(b) C_{d16}T_{e19} : relaxed



(c) C_{d19}T_{e16} : relaxed

FIG .16: Topview of the initial and relaxed geometries